

Scale Invariance and Long-Range Dependence in Smart Energy Grids

Marco Levorato and Urbashi Mitra

Dept. of Electrical Engineering, University of Southern California, Los Angeles, USA.

e-mail: {levorato, ubli}@usc.edu

Abstract—The shift from the traditional energy grid to the SmartGrid makes the features of scale invariance and long-range dependence, traditionally examined in reference to communication networks, extremely relevant to the modeling, analysis and design of modern energy grids. The present paper reviews mathematical concepts and tools central for the understanding and analysis of these phenomena and contextualizes them to the energy scenario. The framework proposed herein enables, in addition to a more accurate modeling and design of smart energy grids, the definition of novel algorithms for the detection of events, e.g., anomalies, in SmartGrids.

I. INTRODUCTION

The SmartGrid [1], [2] is significantly different from the traditional energy grid. The latter is a hierarchical and mono-directional network conveying energy from controllable power plants to consumers. Driven by the need for a reduction of the use of fossil fuels and a more efficient use of the available resources, the SmartGrid incorporates a significant amount of renewable-energy production and pushes intelligence to the edge of the grid. The use of renewable-energy poses novel technological challenges that need to be addressed to guarantee stability of the grid [3]. In fact, whereas the production of fossil fuel-based plants can be planned ahead, the production of renewable energy plants, private or utility-owned, is inherently stochastic, as the amount of energy produced is a function of non-controllable factors such as sun exposure and wind strength. This introduces an additional source of randomness with respect to traditional energy grids, where the principal source of randomness is represented by the demand of energy.

One of the strategies proposed to guarantee stability in this more involved scenario is to increase the level of control on energy consumption by implementing smart algorithms on the demand side [4]. These algorithms react to pricing and control signals by tuning the consumption of individual buildings (smart buildings). In many envisioned frameworks, the algorithms take the form of schedulers storing energy tasks requested by the consumer in a queue and plan the activation of devices according the price of energy and the control signal transmitted by the utility (e.g., [5]–[7]). Similar control rationales are applied to electric vehicle charging, where the acceptance of vehicles and the charging speed is scheduled by algorithms reacting to the load level [8]. Distributed energy production and energy market induce further control-reaction interactions. The dynamics in the SmartGrid, thus, are much more complex than in the traditional energy grid. The framework presented herein is based on two main observations:

- different from the traditional grid, where energy is consumed as the user activate the device, in the SmartGrid, energy consumption is determined by a queueing model, where energy tasks are buffered and then served according to a scheduling algorithm;
- the SmartGrid intelligence is based on a large collection of algorithms actively reacting to events, feedback and control signals.

These intrinsic characteristics of the SmartGrid need to be taken into account for a proper modeling of its operations, as well as for meaningful design of the grid and the algorithms controlling its operations.

The queued service model is significantly different from an instantaneous consumption model. The design and dimensioning of the system (e.g., maximum energy consumption, buffer size) clearly depends on the consumer activity, and affects the Quality-of-Service (QoS) measured at the consumer. Queueing models are also relevant to the energy market and electrical vehicle charging [9], [10]. The complex interactions occurring between the distributed algorithms controlling energy consumption, pricing and energy markets may challenge estimation and detection of critical events in the SmartGrid. In fact, the identification of the dynamics driving the SmartGrid system might require a long observation time and the response of the SmartGrid may be not fast enough to avoid failure. In [11], we proposed a model-detection framework based on wavelet analysis and sparse approximation theory which grants a significant reduction in terms of observation time. In this work, we observe that scaling phenomena may occur in the SmartGrid, and that not only they will affect the performance of the grid, but that they will need to be considered when designing detection frameworks. In fact, algorithms operating on the grid and queueing systems may *rescale* sequences related to events (e.g., failure or anomalous behavior) or inputs (e.g., energy requests).

An intuitive example of rescaling is the smoothing effect of energy schedulers on energy price peaks. A high price induces a reduction of the energy tasks scheduled and an increase of the number of energy requests in the queue. The queued requests are then served at a slower rate until the price decreases. Thus, the number of energy requests in the queue of a scheduler can be seen as a dilated version of the pricing sequence. However, the smoothing effect is also a function of the consumer preferences and external factors such as weather. The queueing process itself can be seen as an intrinsic rescaling of the input sequence generated by

the consumer. Detection and estimation algorithms may be acquiring sequences of measurements associated with rescaled versions of the events and processes they aim to detect and estimate. The use of tools resilient to the rescaling effect is, therefore, crucial to design accurate algorithms.

Connected to the notion of scale, long-range dependence is a key feature in stochastic models for arrival processes. The energy request sequences generated by consumers are likely be driven by stochastic processes inducing long-range dependencies. Individual sources might present long-range dependence due to the strong correlation in the behavior of consumers. At a coarser scale, large aggregates of sources will be affected by long-range dependence. In fact, whereas aggregates of Poisson processes are still Poisson (and thus memoryless), the aggregate of simple On/Off sources with Poisson generation in the On periods present long-term dependencies in the amount of requests in the queue of the schedulers [12]. Long-range dependence deeply affects the performance and stability of the SmartGrid. In fact, long periods of intense generation of energy requests may result in buffer overflow, so that many energy requests generated by the consumers will be lost. Note that peaks in the number of stored requests will also affect delay in their completion. During long periods of no activity, most of the energy tasks requested will be depleted resulting in a low overall load. This may lead to wasting renewable energy resource. The identification of long-range dependence is, then, critical for the design of control sequences such as energy pricing.

The contributions of this paper are

- a review of the notions of self-similarity, scale invariance and long-range dependence, as well as connected mathematical tools such as the Mellin transform;
- a thorough discussion on how self-similarity, scale invariance and long-range dependence will be present in stochastic processes modeling the behavior of the Smart-Grid;
- a review of the tools for the detection of scale invariance and long-range dependence;
- numerical results showing the effect of long-range dependence on the loss rate of energy tasks in a queued energy model.

The rest of the paper is organized as follows. We first review the Mellin transform, the definition of self-similar and scale-invariant stochastic processes and the notion of long-range dependence in Section II and III. We then proceed connecting them to the operations of the SmartGrid. Section V discusses how self-similarity and scale-invariance will characterize the behavior of the SmartGrid. In Section IV, the long-range dependence generated by the aggregation of a large number of On/Off sources generating energy requests is described. Section V discusses the design of tools for estimation and detection of events in the light of the rescaling effect. Numerical results showing the effect of long-range dependence on the congestion level of the grid are presented in Section VI. Section VII concludes the paper.

II. MELLIN TRANSFORM

We first review the Mellin transform [13], a mathematical tool central in the analysis of self-similar and scale-invariant stochastic processes. The Mellin transform of a function f on the positive real axis is defined as

$$\mathcal{M}(f, s) \doteq \int_0^{\infty} f(t)t^{s-1} dt. \quad (1)$$

In general, the function $\mathcal{M}(f, s)$ exists only for complex values of $s=a+jb$ such that $a_1 < a < a_2$, where a_1 and a_2 depend on the function f . The inversion formula is

$$f(t) = \frac{1}{2j\pi} \int_{a-j\infty}^{a+j\infty} \mathcal{M}(f, s)t^{-s} ds. \quad (2)$$

The Mellin transform has been introduced primarily to handle harmonic sums of the kind

$$\sum_{i \geq 0} c_i f(\omega_i t) \quad (3)$$

for some sequences c_i and ω_i such that the sum is convergent. The transform of the harmonic sum is

$$\left(\sum_{i \geq 0} c_i \omega_i^{-s} \right) \mathcal{M}(f, s)(s). \quad (4)$$

Moreover, the asymptotic analysis of a function $f(t)$ when t tends to 0 and ∞ is equivalent to the analysis of the singularities of the Mellin transform $\mathcal{M}(f, s)(s)$ on the boundaries of the strip where the transform exists. As explained later, this property is relevant in the analysis of the queue length distribution, and thus on the delay analysis, of energy tasks in the On/Off sources scenario. The Mellin transform is a powerful tool for the computation of functionals involving the scaling of a variable. Define the dilation operator

$$\mathcal{D}_c^r : f(t) \rightarrow (\mathcal{D}_c f)(t) = c^{r+1} f(ct), \quad (5)$$

where c is a positive number and r is a given real number. We have

$$\mathcal{M}(\mathcal{D}_c f, \beta) = r^{-2\pi j\beta} \mathcal{M}(f, \beta), \quad (6)$$

where, referring to the definition in Eq. (1)

$$s - 1 = 2\pi j\beta + r. \quad (7)$$

III. STOCHASTIC SELF-SIMILARITY, SCALE INVARIANCE AND LONG-RANGE DEPENDENCE

In this section, we review the notions of self-similarity, scale invariance and long-range dependence in stochastic processes. These features will occur in stochastic processes modeling the behavior of the SmartGrid and influence the Quality-of-Service offered to consumers.

Self-similarity expresses the notion that a certain property of an object or a dynamical system is preserved with respect to scaling in space and/or time. Stochastic self-similarity measures the similarity of certain statistics of rescaled stochastic processes. The autocorrelation function is an example of a statistic with respect to which scale invariance can be defined. Considering the finite dimensional distributions of continuous processes, the definition of self-similarity is as follows.

Definition 1 A process $X(t)$ is self-similar with self-similarity parameter H (H -ss), $0 < H < 1$ if, for all $r > 0$ and $t > 0$ we have

$$X(t) \stackrel{d}{=} r^{-H} X(rt), \quad (8)$$

that is, $X(t)$ and its time scaled and normalized version $r^{-H} X(rt)$ have the same distribution.

Interestingly, there is a strong connection between self-similarity and stationarity: this result is referred to as the Lamperti theorem [14] and can be stated as follows:

Theorem 2 If $\{X(t), t \in \mathbb{R}^+\}$ is H -ss, then

$$Y(t) = e^{-Ht} X(e^t), \quad t \in \mathbb{R}, \quad (9)$$

is stationary. Conversely, if $\{Y(t), t \in \mathbb{R}^+\}$ is stationary, then

$$X(t) = t^H Y(\log(t)) \quad (10)$$

is H -ss.

The central argument of the derivation of the Lamperti theorem is that the Lamperti transform [14] maps a time-shifted process to the dilated version of the Lamperti transform and vice-versa, where the Lamperti transform is defined as

$$(\mathcal{L}X)(t) \doteq t^H X(\log(t)), \quad t \in \mathbb{R}^+, \quad (11)$$

$$(\mathcal{L}^{-1}X)(t) \doteq e^{-Ht} X(e^t), \quad t \in \mathbb{R}. \quad (12)$$

There is a strong connection between Fourier, Lamperti and Mellin transforms. We have

$$\mathcal{F}(X)(f) = \mathcal{M}(\mathcal{L}_H X, H + 2j\pi f). \quad (13)$$

Thus, in the case of a self-similar process the Mellin transform has a similar effect with respect to scaling than the Fourier transform has with respect to shifting.

A weaker form of self-similarity, namely discrete self-similarity, was introduced in [15]. A process $\{X(t), t \in \mathbb{R}^+\}$ has Discrete Scale Invariance (DSI) with scaling exponent H and scale λ ((H, λ) -DSI) if

$$X(\lambda t) \stackrel{d}{=} \lambda^{-H} X(t), \quad (14)$$

In [15] it is shown that if a process is (H, λ) -DSI, then its Lamperti transform is cyclostationary and vice-versa. However, self-similarity can be defined on second-order statistics.

Definition 3 $X(t)$ is exactly second-order self-similar with parameter H , $1/2 < H < 1$ if

$$\gamma(k) = \frac{\sigma^2}{2} ((k+1)^{2H} - sk^{2H} + (k-1)^{2H}), \quad (15)$$

for all $k \geq 1$. $X(t)$ is asymptotically second-order self-similar if

$$\lim_{m \rightarrow \infty} \gamma^{(m)}(k) = \frac{\sigma^2}{2} ((k+1)^{2H} - sk^{2H} + (k-1)^{2H}), \quad (16)$$

where $\sigma^2 = E[(X(t) - \mu)^2]$, $\mu = E[X(t)]$, $\gamma(k)$ is the autocovariance of $X(t)$ and $\gamma^{(m)}(k)$ is the autocovariance of

$$X^{(m)}(q) = \frac{1}{m} \sum_{t=m(q-1)+1}^{mq} X(t). \quad (17)$$

Note that $X^{(m)}$ is the process corresponding to the average of $X(t)$ over time intervals of size m .

As explained later, the algorithms operating in the SmartGrid may have a re-scaling effect

A feature strongly connected to self-similarity is long-range dependence:

Definition 4 The process $X(t)$ is long-range dependent if its autocorrelation function $r(k) = \gamma(k)/\sigma^2$ is not summable

$$\sum_{k=-\infty}^{+\infty} r(k) = \infty. \quad (18)$$

If $X(t)$ is second-order self-similar with parameter $1/2 < H < 1$ then $r(k)$ asymptotically behaves as $ck^{-\beta}$, with $c > 0$ and $0 < \beta < 1$, and the process is long-range dependent [16]. Long-range dependence induces strong correlation in the behavior of a stochastic process. As explained later in the paper, in the SmartGrid, long-range dependence in the generation of energy requests by consumers can lead to poor performance in terms of delay in the completion of the energy tasks and a high loss rate due to buffers overflow.

IV. ENERGY QUEUEING WITH ON/OFF SOURCES

The queueing model that characterizes the SmartGrid may significantly change the properties of the stochastic process modeling energy consumption. Understanding the characteristics of these processes is crucial to properly designing the system and measuring the performance at the consumer. The overall consumption is the result of a large number of individual smart buildings and homes¹ controlled by automated systems. Fig. 1 shows the schematic of a smart home. Energy requests triggered by the consumer are collected in a queue. The scheduler then controls the activation of the appliances as a function of energy pricing and grid signaling. Constraints can be included in the model to force the activation of specific appliances. Quality of Service can be measured as a function of delay of activation and financial cost.

Self-similar bursts of traffic and memory effects were measured in internet traffic (e.g., [18]). In particular, long-range dependence was identified in the traffic traces. Self-similarity and long-range dependence can be caused by a heavy-tailed distribution of the tasks to be deployed by the server. However, in [19] it was shown that an aggregation of sources with memoryless profiles can also generate long-dependence effects. Poisson processes are widely used to model arrival processes as the resulting frameworks are easily analyzable. The Poisson process is generated by the aggregation of N i.i.d. random processes generating events at rate λ/N for N asymptotically large. The distribution of the interarrival time τ is then

$$P(\tau > x) = e^{-\lambda x}. \quad (19)$$

Consider a consumer generating energy requests whose duration is exponentially distributed according to a Poisson process with intensity λ . If the service rate is equal to 1 and the buffer

¹As well as a smaller number of, more predictable, industry sites.

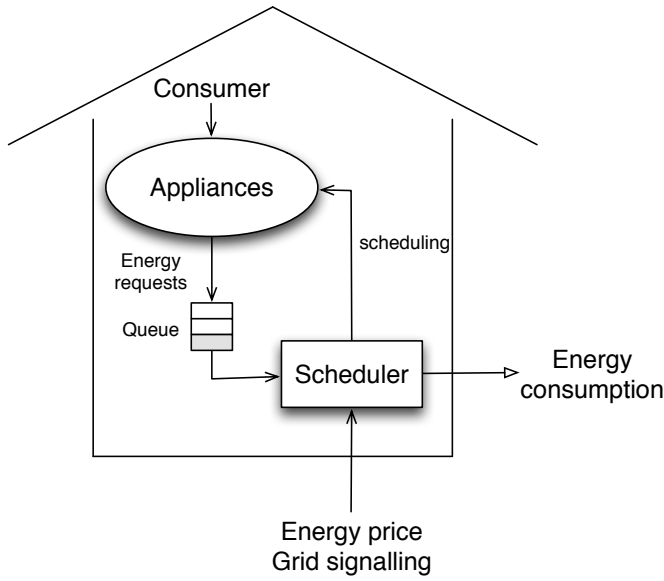


Fig. 1. Schematics of a smart home: the consumer activates appliances, that generate energy requests queued in a buffer. The energy tasks are scheduled as a function of energy pricing and grid signaling. The output of the scheduler determines the overall demand to the grid and is fed-back to the appliances.

is infinite, then the probability that the number of tasks to be completed and stored in the queue is larger than n is λ^n . The distribution of the queue length is related to the delay between by the Little's law [17]:

$$W = \frac{\bar{Q}}{\lambda}, \quad (20)$$

where W is the average waiting time in the queue and Q is the average queue length. Queuing processes with Poisson arrivals have good properties as the distribution of the queue size exponentially decays. However, the generation of energy requests is unlikely follow a simple Poisson process.

Consider now the On/Off source model described as follows (Fig. 2):

- the transition from On to Off and Off to On occurs with probability v_0 and v_1 , respectively (the length of On and Off periods are exponentially distributed);
- in the On period the source generate energy requests with rate λ ;
- in the Off period the source generate energy requests with rate 0.

Even if the individual source is memoryless, the aggregate of a large number of these sources induces long-range dependence for some ranges of parameters. As observed in [12], buffering the tasks generated by a large collection of these sources results in a polynomial distribution of the queue length. As a consequence, *the buffer needs to be much larger than in*

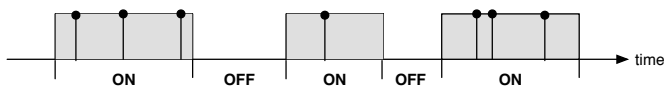


Fig. 2. On/Off source model. Grey regions correspond to On periods. Dots represent energy tasks arrivals.

the pure Poisson case to have the same probability of buffer overflow, and the average delay considerably increases. The Mellin transform is central in the analysis of the statistics of the queue in [12]. In [12], the Mellin transform is used to derive the asymptotic behavior of the aggregate of sources.

These considerations are of particular interest in the Smart-Grid scenario, where the overall energy demand is generated by a very large number of sources. Although the On/Off source model described before may not perfectly fit the generation of energy demands, it enlightens the fact that bursty activity, that is likely to characterize a key part of the energy demand generation, induces correlation in scenarios with a large number of sources. We will show in Section VI that long-range dependence deeply impacts the performance of queued SmartGrid system. This effect needs to be considered when designing the provided service rate, and the peak consumption.

V. SELF-SIMILARITY, RESCALING AND ESTIMATION IN THE SMARTGRID

The scaling phenomena widely observed in telecommunication networks will occur in SmartGrid systems. The interaction between generation of energy requests, energy tasks queueing and scheduling, energy pricing can induce rescaling of input processes when observed in other domains. The scenario introduced in the previous section is emblematic: the large number of sources generating energy demand can induce self-similarity and long-dependence even if the individual source is memoryless. However, another important application is the detection of rescaling to estimate properties of the original *input* signals. Load controllers and smart home schedulers *filter* input sequences such as pricing and energy requests, that in turn may be functions of other *events* in the grid. For instance, the size of the queue of the scheduler is a rescaled version of the input sequence of energy requests where the dilation function is determined by external factors such as energy pricing. Note that while self-similarity of energy demand induces scale invariance, rescaling due to queueing and dilation may involve a given scale or induce DSI.

The identification of scaling behavior is crucial. In fact, by detecting the presence or absence of scaling, one can decide whether measurements should be analyzed with traditional techniques or with methodologies accounting for the presence of scaling. This section discusses estimation of the scale of self-similar and DSI processes.

A. Mellin-based Methods

In [15] an interesting framework is proposed for the analysis of DSI processes based on the Mellin transform. The Lamperti transform connects the dilation operator to a time-shift operator. In fact,

$$(\mathcal{L}^{-1} \mathcal{D}_\lambda^{-r+1} \mathcal{L} X)(t) = (\mathcal{S}_{\log \lambda} X)(t), \quad (21)$$

where

$$(\mathcal{S}_T X)(t) = X(t + T). \quad (22)$$

The Lamperti transform of DSI processes, then, is a cyclostationary process and vice-versa, and the correlation function

$$R(t, \tau) = E[X(t)X(\tau)] \quad (23)$$

of (H, λ) -DSI processes has the Fourier series expansion

$$R(t, kt) = k^H t^{2H} \sum_{n=-\infty}^{+\infty} C_n(k) t^{\frac{2j\pi n}{\log \lambda}}. \quad (24)$$

Based on these observations, [15] proposed a decomposition in scale of the correlation function of multiplicative harmonizable processes where the following holds:

$$R(t, \tau) = \int \int t^{H+2j\pi\beta} \tau^{H-2j\pi\sigma} \Phi(\sigma, \beta) d\sigma d\beta. \quad (25)$$

The spectral distribution $\Phi(\sigma, \beta) d\sigma$ can be found as the inverse Mellin transform of Eq. (24) if $R(t, \tau)$ is known, that is

$$\Phi(\sigma, \beta) = \int \int t^{-H-2j\pi\beta} s^{-H+2j\pi\sigma} R(t, \tau) \frac{dt d\tau}{t\tau}. \quad (26)$$

The following holds

$$\Phi(\sigma, \beta) = \sum_{n=-\infty}^{\infty} \tilde{C}_n(\sigma) \delta(\beta - \gamma - \frac{n}{\log \lambda}), \quad (27)$$

where $\tilde{C}_n(\sigma)$ is the Mellin transform of $C_n(k)$. In fact, harmonizable cyclostationary processes have spectral function non-zero only on parallel lines where $\nu - f = n/T$, and T is the period of the process.

Based on these results, a series of methods based on the Mellin transform for the estimation of the scaling parameter λ and of the correlation function are proposed in [15]. As the Mellin transform is weakly sensitive to the amplitude factor r , one can use $r=1/2$ in the Mellin transform and obtain spreaded versions of Dirac function in the transform. The multiplicative spectral function in Eq. (27) can be used to formulate a scale-decomposition similar to the time-frequency decomposition in [20] for the estimation of the correlation function. The parameter λ can be retrieved by using an estimate of $\Phi(\sigma, \beta)$ to compute the peak of the marginal [15]

$$\int \Phi(\nu - \frac{\beta_c}{2}, \nu + \frac{\beta_c}{2}). \quad (28)$$

The coefficients $\tilde{C}_n(\sigma)$ in the resulting decomposition can be constructed as in [21].

B. Wavelets-based Methods

Wavelets-based approaches can be used for the identification of scaling behavior and the estimation of the scaling parameter [16], [22]. Wavelet families possess a scale-invariant construction and, thus, are suitable for the analysis of scaling phenomena. Multi-Resolution Analysis provides a representation of a signal $X(t)$ as

$$X(t) = \sum_{j,k} C_{j,k} \phi_{\beta,\tau}(t), \quad (29)$$

where $\phi_{j,k}$ is a scaled and shifted version of the mother wavelet function ϕ_0 of the form

$$\phi_{j,k}(t) = 2^{-j/2} \phi_0(2^{-j}t - k), \quad (30)$$

and $C_{j,k} = \langle \phi_{j,k}, X \rangle$. If $X(t)$ is a self-similar process with parameter H , the coefficients $C_{\beta,\tau}$ exactly reproduce self-similarity [22]:

$$C_{j,k} = 2^{j(H+1/2)} C_{0,k}. \quad (31)$$

The wavelet coefficients with a fixed scale coefficient j form a stationary process [22]. If $X(t)$ is second-order self-similar with parameter H then the coefficients located at different positions are small as soon as $N > H+1/2$, where N is the number of vanishing moments of ϕ_0 [16]. In particular, the following holds:

$$E[C_{j,k} C_{j',k'}] \sim |2^j k - 2^{j'} k'|^{2H-2N}, \quad |2^j k - 2^{j'} k'| \rightarrow \infty. \quad (32)$$

The advantage of building estimators in the wavelet domain, instead of operating in the time domain, is that the coefficients $C_{j,k}$ are short-range stationary processes weakly dependent among themselves. In this representation, the scaling coefficient is the slope of the log-log plot of

$$\mu_j = \frac{1}{n_j} \sum_{k=1}^{n_j} |C_{j,k}|^2 \quad (33)$$

on the scale j . Details are provided in [16].

VI. NUMERICAL RESULTS

In this section, we present numerical results showing the impact of long-range dependence on a queued energy system with multiple sources generating energy requests. Long-range dependence² significantly affect the evolution of the queue and, thus, the performance of the system. In fact, long bursts of activity of the sources may result in buffer overflow, whereas long bursts of inactivity may lead to periods with very low energy consumption and, thus, waste of available renewable resources. Algorithms detecting the presence of long-range dependence are, therefore, critical for the correct design of control sequences (*e.g.*, energy pricing) that, by influencing the scheduling of energy tasks, influence the temporal evolution of the SmartGrid system.

The schematic of the considered system is depicted in Fig. 3. A set of N On/Off sources submit energy tasks to a scheduler. During their On period, the sources generate energy tasks according to a Poisson distribution with rate η . The energy tasks are queued in a finite First-Input First-Output queue of size Q . In each time unit, the scheduler serves a number of units of energy distributed according to a Poisson distribution whose rate depends on the price of energy. The temporal evolution of the energy price is modeled as a Markov process in order to capture temporal correlation. This system emulates a basic queued energy system where the load, that is, the energy spent per unit of time, is controlled by the price of energy. The model can be applied to different scales of the SmartGrid. A small number of sources presenting strong long-range dependence can be seen as an individual building where sources are appliances and the scheduler is a residential Demand Response system. At a larger scale, a large number of sources can be seen as a collection of buildings generating requests of allocation of energy to a micro-grid controller.

²We remark that long-range dependence and self-similarity are strongly connected.

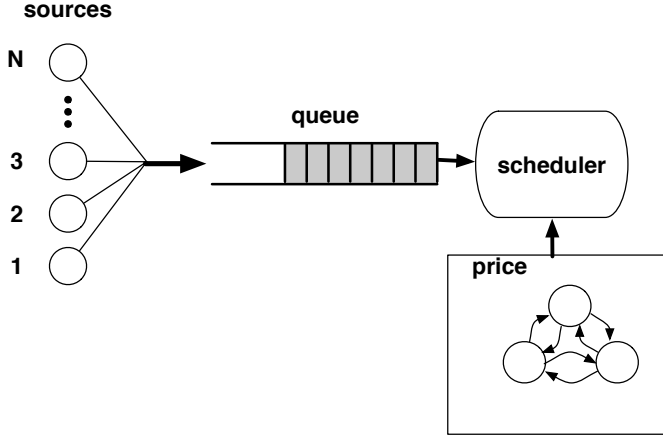


Fig. 3. Schematic of the system: N sources submit energy tasks to the queue of the scheduler. The service rate of the scheduler is a function of the energy price, whose evolution is modeled as a Markov process.

In order to assess the impact of long-range dependence we consider two cases. In the first case the On/Off periods of the sources are exponentially distributed with parameter λ_{on} and λ_{off} , respectively. Thus, the probability that the duration $I_{\text{On(Off)}}$ of an On(Off) interval is smaller than x is

$$F_{\text{exp}}(x) = P(I_{\text{On(off)}} \leq x) = 1 - e^{-\lambda_{\text{on(off)}}x}. \quad (34)$$

The exponential distribution is memoryless, that is:

$$P(I_{\text{On(off)}} > x + x' | I_{\text{On(off)}} > x) = P(I_{\text{On(off)}} > x'). \quad (35)$$

In the second case, we consider On/Off intervals distributed according the Pareto distribution. Then, we have

$$F_{\text{pareto}}(x) = P(I_{\text{on}} \leq x) = 1 - \left(\frac{k_{\text{on}}}{x}\right)^{\alpha_{\text{on}}}. \quad (36)$$

An analogous expression can be written for the Off intervals.

The Pareto distribution is a heavy-tailed distribution and presents long-range dependence and self-similarity. The parameter $\alpha_{\text{on/off}}$ and k are called the shape and scale parameters, respectively. If $\alpha_{\text{on/off}} \leq 1$, then the intervals have infinite mean. If $\alpha \leq 2$, then the intervals have infinite variance. Note that $\alpha_{\text{on/off}}$ is related with the Hurst parameter H . In fact, $H = (3 - \alpha_{\text{on/off}})/2$.

TABLE I
SIMULATION PARAMETERS

Parameter	Value
N	2
η	$1/N$
$\alpha_{\text{on}} = \alpha_{\text{off}}$	1.2
$k_{\text{on}} = k_{\text{off}}$	1.2
Q	40
$p(\text{low}, \text{low})$	0.8
$p(\text{high}, \text{high})$	0.8
μ_{low}	0.6
μ_{high}	3

In order to have a fair comparison, we set $\alpha_{\text{on}}, \alpha_{\text{off}} > 1$ and we fix

$$\lambda_{\text{on}}^{-1} = k_{\text{on}} \frac{\alpha_{\text{on}}}{1 - \alpha_{\text{on}}}, \quad (37)$$

$$\lambda_{\text{off}}^{-1} = k_{\text{off}} \frac{\alpha_{\text{off}}}{1 - \alpha_{\text{off}}}. \quad (38)$$

Thus, the average duration of the intervals is the same in the two cases. Thus, in the two cases, the sources generate the same amount of energy tasks on average. Numerical results show that even if the number of generated energy tasks is the same, long-range dependence results to a larger number of energy tasks lost due to a full buffer. We also observe that long-range dependence also results to a larger delay in the completion of the tasks and may lead to consumers dissatisfaction.

In the numerical results, we consider a binary *low/high* price sequence. The scheduler serves the energy tasks at rate μ_{low} and μ_{high} if the price is low or high, respectively. The statistics of the sequence are determined by a Markov process with transition probability matrix

$$\begin{pmatrix} p(\text{low}, \text{low}) & 1 - p(\text{low}, \text{high}) \\ 1 - p(\text{high}, \text{low}) & p(\text{high}, \text{high}) \end{pmatrix}, \quad (39)$$

where $p(\text{low}, \text{low})$ and $p(\text{high}, \text{high})$ are the probabilities that the process remains in the low price state and in the high price state, respectively. The generation rate is set to $\eta = 1/N$. Thus, the generation rate is split among the sources as N increases, and on average the same amount of energy requests is generated for any N . The value of the parameters are listed in Table I unless specified otherwise in the figures.

Fig. 4 shows the overall number of energy tasks lost due to buffer overload in a scenario with 2 sources. It can be observed that On/Off intervals with Pareto distribution generates a much larger number of discarded energy tasks than On/Off intervals with exponential distribution. This is due to the heavy-tail of the Pareto distribution. In fact, the heavy-tale, that is, non-negligible probability of very large intervals, correlates the On/Off process. Thus, there is a larger probability that a source persists in the On or Off state with respect to the exponential distribution. During a long On interval, the price sequence may hit a period of high price state, where the scheduler can complete the energy tasks at a slower rate than their arrival rate. In this case, the buffer may fill and energy tasks may be discarded due to buffer overload. Long Off intervals may only partially reduce this effect, as the scheduler may empty the queue and lose available energy resources.

Fig. 5 shows the overall number of energy tasks lost due to buffer overload in a scenario with 40 sources. We remark that the arrival rate of the energy tasks is split among the sources, so that the overall load is the same. The overall number of energy tasks lost is much smaller than in the case $N=2$. In fact, a larger number of *lighter* sources produces a more homogeneous arrival process. Thus, the scheduler can continuously serve energy tasks and whole the available resource is used. Moreover, the gap between the Pareto and exponential distribution is smaller. In fact, a large number of memoryless sources may generate long range dependence. Thus, even in the large scale, the design of the dimension of the

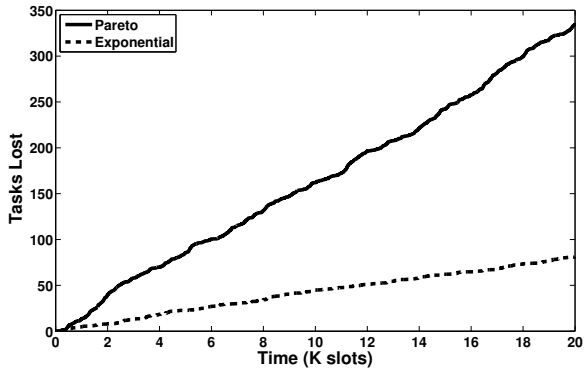


Fig. 4. Number of tasks lost as a function of time for the Pareto and exponential distribution. The number of sources is equal to 2.

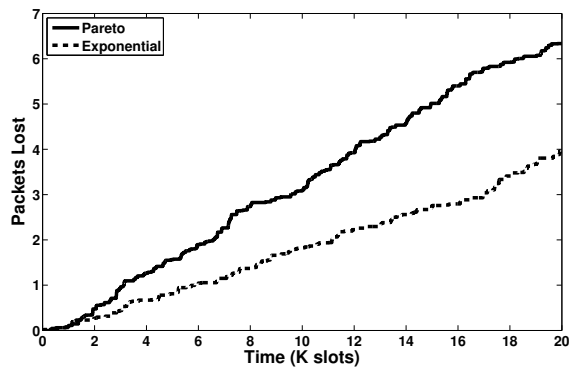


Fig. 5. Number of tasks lost as a function of time for the Pareto and exponential distribution. The number of sources is equal to 40.

buffer must take into account this effect. Fig. 6, where the loss rate of the energy tasks is depicted as a function of the number of sources, further corroborates these two observations.

Finally, Fig 7 shows the loss rate of the energy tasks as a function of the shape parameter α . We remark that α is related to the Hurst parameter, and thus, to the long-range dependence of the On/Off intervals. It can be observed that the long-range effect vanishes as α is increased.

These results show the impact of long-range dependence and self-similarity of the functioning of the SmartGrid. A controller aware of the presence of these phenomena can design the energy pricing sequence in order to avoid buffer overflow and low energy usage periods. We leave the design of scale and long-range detectors and of the pricing strategies to future work.

VII. CONCLUSIONS

A discussion on the relevance of scale invariance, self-similarity and long-range dependence in SmartGrid systems. The interaction between input sequences such as energy requests, pricing, and physical and control systems can induce rescaling effects that need to be considered when designing estimation algorithms. Moreover, long-range dependence can arise when a large collection of On/Off memoryless sources contributes to the generation of energy requests. The estimation of the parameters characterizing these processes and

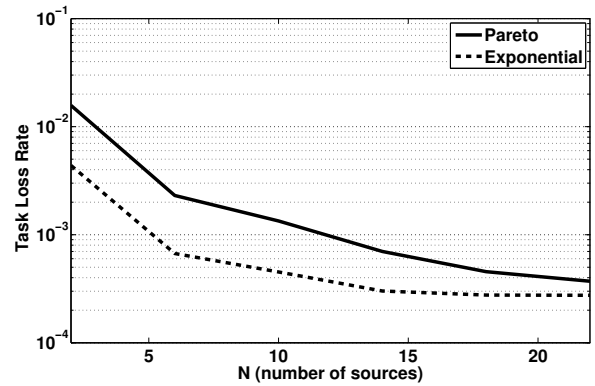


Fig. 6. Task loss rate as a function of the number of sources for the Pareto and exponential distribution.

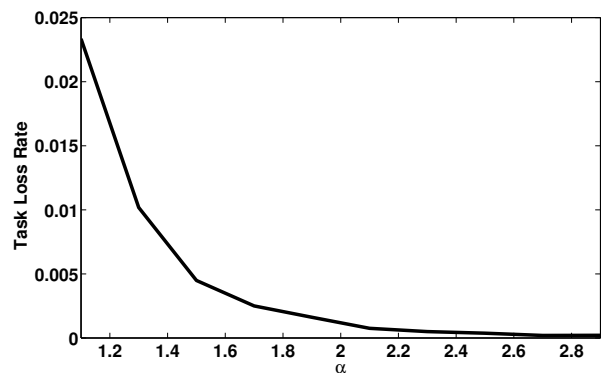


Fig. 7. Task loss rate as a function of the shape parameter α . The number of sources is equal to 2.

effects is critical for a proper dimensioning of the system and the detection of failures and anomalies. A detailed discussion on estimation frameworks for was provided. Numerical results show that long-range dependence significantly affect the performance of the SmartGrid system. The detection of scaling phenomena is, therefore, critical for designing effective control strategies.

REFERENCES

- [1] C. Shuyong, S. Shufang, L. Lanxin, and S. Jie, "Survey on smart grid technology," *Power Sys. Tech.*, vol. 33, no. 8, pp. 1–7, 2009.
- [2] R. Brown, "Impact of Smart Grid on distribution system design," in *Power and Energy Society General Meeting-Conversion and Delivery of Electrical Energy in the 21st Century, 2008 IEEE*. IEEE, 2008, pp. 1–4.
- [3] A. Mohd, E. Ortjohann, A. Schmelter, N. Hamsic, and D. Morton, "Challenges in integrating distributed energy storage systems into future smart grid," in *Industrial Electronics, 2008. ISIE 2008. IEEE International Symposium on*. IEEE, 2008, pp. 1627–1632.
- [4] K. Kok, S. Karnouskos, D. Nestle, A. Dimeas, A. Weidlich, C. Warmer, P. Strauss, B. Buchholz, S. Drenkard, N. Hatzigiorgiour, and V. Lioliou, "Smart houses for a smart grid," in *20th International Conference and Exhibition on Electricity Distribution*, june 2009, pp. 1 –4.
- [5] D. O'Neill, M. Levorato, A. Goldsmith, and U. Mitra, "Residential Demand Response Using Reinforcement Learning," in *IEEE SmartGridComm*. IEEE, 2010, pp. 409–414.
- [6] L. Ying and M. Trayer, "Automated residential demand response: Algorithmic implications of pricing models," in *2012 IEEE International Conference on Consumer Electronics (ICCE)*, Jan. 2012, pp. 626 –629.

- [7] K. C. Sou, J. Weimer, and K. H. J. H. Sandberg, "Scheduling smart home appliances using mixed integer linear programming," in *50th IEEE Conference on Decision and Control and European Control Conference*, Dec. 2011.
- [8] A. Brahma, Y. Guezennec, and G. Rizzoni, "Optimal energy management in series hybrid electric vehicles," in *American Control Conference, 2000. Proceedings of the 2000*, vol. 1, no. 6. IEEE, 2000, pp. 60–64.
- [9] A. Scaglione, M. Alizadeh, and R. J. Thomas, "Queuing models for providing quality of service to transactive loads," in *IEEE PES - Innovative Smart Grid Technologies*, jan. 2012.
- [10] M. Alizadeh, A. Scaglione, and R. J. Thomas, "Direct load management of electric vehicles," in *IEEE International Conference on Acoustics, Speech and Signal Processing (ICASSP)*, may 2011, pp. 5964–5967.
- [11] M. Levorato and U. Mitra, "Fast anomaly detection in smartgrids via sparse approximation theory," in *IEEE 7th Sensor Array and Multichannel Signal Processing Workshop (SAM)*, june 2012, pp. 5–8.
- [12] P. Jacquet, "Long term dependences and heavy tails in traffics and queues generated by memoriless on/off sources in series," in *Rapport de recherche - Inst. Nat. de Recherche en Informatique et en Automatique*, no. 3516, 1998.
- [13] J. Bertrand, P. Bertrand, and J. P. Ovarlez, "The mellin transform," *ONERA, TP no. 1994-98*, 1994.
- [14] J. Lamperti, "Semi-stable stochastic processes," *Trans. Amer. Math. Soc.*, vol. 104, pp. 62–78, 1962.
- [15] P. Borgnat, P. Flandrin, and P.-O. Amblard, "Stochastic discrete scale invariance," *IEEE Signal Processing Letters*, vol. 9, no. 6, pp. 181–184, jun. 2002.
- [16] K. Park and W. Wellinger, *Self-similar Network Traffic and Performance Evaluation*. John Wiley & Sons, Inc, 2000.
- [17] J. D. C. Little and S. C. Graves, "Little's law," in *Building Intuition*, ser. International Series in Operations Research & Management Science. Springer US, 2008, vol. 115, pp. 81–100.
- [18] M. Crovella and A. Bestavros, "Self-similarity in world wide web traffic: Evidence and possible causes," in *ACM SIGMETRICS*, May 1996.
- [19] K. Park and W. Wellinger, *Statistics for Long Memory Processes*. John Wiley & Sons, Inc, 2000.
- [20] P. Flandrin, *Time-Frequency/Time-Scale Analysis*. New York Academic, 1999.
- [21] D. Dehay and H. Hurd, *Stochastic discrete scale invariance*. in *Cycl. in Communications and Signal Processing*, W. Gardner, Ed. Piscataway, NJ: IEEE Press, 1994.
- [22] L. Delbeke, *Wavelet Based Estimators for the Scaling Index of a Self-Similar Process with Stationary Increments*. Ph.D. thesis, KU Leuven, Belgium, 1998.